NEUROPROSTHETICS

Proprioception from a neurally controlled lower-extremity prosthesis

Tyler R. Clites,[1,2] Matthew J. Carty,[1,3] Jessica B. Ullauri,[1] Matthew E. Carney,[1,4] Luke M. Mooney,[1] Jean-François Duval,[1] Shriya S. Srinivasan,[1,2] Hugh. M. Herr[1,2,3,4]*

Humans can precisely sense the position, speed, and torque of their body parts. This sense is known as proprioception and is essential to human motor control. Although there have been many attempts to create human-mechatronic interactions, there is still no robust, repeatable methodology to reflect proprioceptive information from a synthetic device onto the nervous system. To address this shortcoming, we present an agonist-antagonist myoneural interface (AMI). The AMI is composed of (i) a surgical construct made up of two muscle-tendons—an agonist and an antagonist—surgically connected in series so that contraction of one muscle stretches the other and (ii) a bidirectional efferent-afferent neural control architecture. The AMI preserves the dynamic muscle relationships that exist within native anatomy, thereby allowing proprioceptive signals from mechanoreceptors within both muscles to be communicated to the central nervous system. We surgically constructed two AMIs within the residual limb of a subject with a transtibial amputation. Each AMI sends control signals to one joint of a two-degree-of-freedom ankle-foot prosthesis and provides proprioceptive information pertaining to the movement of that joint. The AMI subject displayed improved control over the prosthesis compared to a group of four subjects having traditional amputation. We also show natural reflexive behaviors during stair ambulation in the AMI subject that do not appear in the cohort of subjects with traditional amputation. In addition, we demonstrate a system for closed-loop joint torque control in AMI subjects. These results provide a framework for integrating bionic systems with human physiology.

INTRODUCTION

Proprioception is the sense of the relative spatial positioning of one's body parts and of the amount of force exerted on the environment (1). It is essential to human motor control, gait adaptation, and joint stability (2, 3). In humans, proprioceptive feedback is primarily mediated by a complex relationship between sensory organs within muscles and tendons (1). Although a large body of literature exists surrounding the biological structures involved in proprioceptive sensation, including stretch receptors in the skin (4–6) and movement receptors in the joints (7–9), there is substantial evidence highlighting muscle spindles and Golgi tendon organs (10) as the predominant mediators of joint proprioception (1). Muscle spindles and Golgi tendon organs represent only a portion of the larger proprioceptive system; however, studies in vibration-induced illusory kinesthesia have indicated that isolated activation of muscle afferent receptors is sufficient to promote sensations of joint position, movement, and torque (11, 12). Further evidence indicates that the dynamic relationships within agonist-antagonist muscle pairs are fundamental to natural sensations of joint movement (13). The complexity of this afferent (neural pathways that relay information from a muscle or other end organ to the central nervous system) feedback system poses a challenging hurdle for the development of bionic limbs that benefit from bidirectional neural communication.

The clinical standard of care for limb amputation surgery has not changed in almost two centuries and is not currently optimized to facilitate neural integration with bionic limbs. In a typical amputation procedure, muscle tissues in the residual limb are configured isometrically to create padding for a prosthetic socket (14), severing the dynamic relationship between agonist-antagonist muscle pairs and limiting the ability of the muscle spindles and Golgi tendon organs within these tissues to communicate meaningful information to the central nervous system. Muscles, tendons, skin, bones, and other tissues distal to the amputation site are typically discarded, despite their potential capacity to contribute to reconstruction of the amputated residuum. Nerves that cross the amputation boundary are cut under tension and then buried into fat tissue or deep in the residuum in an effort to prevent the formation of inappropriate nerve tissue growths, called neuromas, which can cause pain or other phantom sensations (15). Although sometimes effective in preventing neuropathic pain, this technique creates a hurdle for neural interfaces because of the limited longitudinal viability of direct contact between synthetic interfaces and peripheral nerve tissues, especially for neural recording (16, 17). Robotic prostheses have been designed around these limitations and fall short of reproducing the biological control experience. The present state-of-the-art commercial technology for persons with below-knee amputation is a powered ankle joint that is unable to fully reproduce the motions of the biological ankle and subtalar joints and does not have any direct connection to the nervous system (18).

Many attempts have been made to overcome the limitations of state-of-the-art amputation surgical techniques and commercial prosthetic systems. Direct stimulation of upstream peripheral nerves through implantable electrodes has shown great promise in restoring cutaneous touch perception and, in some cases, isolated kinesthetic sensations (19–25). However, partly because of a mismatch between the complexity of proprioceptive afferent signaling and the relatively low resolution and precision of implantable stimulation methodologies, none of these approaches is engineered to provide, with high-probability, stable and natural proprioceptive percepts. Vibration-induced illusory kinesthesia (12) has been explored as a means of providing joint state

[1]Center for Extreme Bionics, Massachusetts Institute of Technology (MIT) Media Lab, Cambridge, MA 02139, USA. [2]Harvard–MIT Division of Health Sciences and Technology, MIT, Cambridge, MA 02139, USA. [3]Division of Plastic and Reconstructive Surgery, Brigham and Women's Hospital, Boston, MA 02115, USA. [4]Department of Media Arts and Sciences, MIT, Cambridge, MA 02139, USA.
*Corresponding author. Email: hherr@media.mit.edu

information through activation of cutaneous stretch receptors; unfortunately, translation of this approach has been a major hurdle. Regenerative peripheral nerve interfaces have emerged as a means of stifling neuroma formation, preventing phantom pain, increasing the number of independent neural control targets, and conveying cutaneous sensory information (26, 27). Targeted muscle reinnervation has a strong track record of improving controllability of myoelectric prostheses but is not designed to close the control loop with proprioceptive sensation (28, 29). Prosthetic hardware has also seen dramatic improvement in recent years (29–35), including substantial improvements to myoelectric control architectures (20, 27–29, 34, 36).

As a methodology of improving efferent (neural pathways that relay commands from the central nervous system to a muscle or other end organ) prosthetic control and providing afferent proprioceptive sensation, we present an agonist-antagonist myoneural interface (AMI). An AMI is made up of an agonist and an antagonist muscle-tendon connected mechanically in series: When the agonist contracts, the antagonist is stretched and vice versa (37, 38). The purpose of an AMI is to control and interpret proprioceptive feedback from a bionic joint. This approach was first validated in several experiments using animal models. An AMI was constructed from musculature with intact innervation and vascular supply in a rat distal hindlimb (39). Graded afferent signals were then recorded from the agonist muscle's innervation nerve during closed-loop functional electrical stimulation of the antagonist, demonstrating the capacity of the AMI to provide natural proprioceptive feedback. In another murine study, we demonstrated that a functional AMI could be constructed from small denervated and devascularized muscle grafts placed in the vicinity of transected motor nerves (40). A caprine experiment further validated that the principles demonstrated in (39) are scalable to larger animal models (41).

On the basis of these previous studies, we hypothesized that the AMI procedure and rehabilitation protocol would enable improved control of a multi-degree-of-freedom prosthesis while reflecting natural proprioceptive sensation pertaining to each prosthetic joint onto the central nervous system. In the case study presented herein, we test this hypothesis in a human subject having a unilateral transtibial amputation. We first describe the implementation of two AMIs within the subject's residuum and connection via synthetic electrodes to an external prosthetic leg with powered artificial ankle and subtalar joints. The ability of this AMI patient (subject A) to volitionally and reflexively control the prosthesis in free space was evaluated and compared to a cohort of four participants having traditional transtibial amputation (group T, composed of subjects T1 to T4). We conclude with an evaluation of a functional electrical stimulation (FES) methodology for providing torque feedback from a prosthesis to the peripheral nervous system of subject A.

RESULTS
AMI surgical construction
Two AMIs were constructed in the residual limb of a 53-year-old male at the time of his elective unilateral transtibial amputation. One AMI, composed of the tibialis posterior and the peroneus longus, was designed to control the bionic subtalar joint responsible for prosthetic inversion and eversion movements (Fig. 1, A1 and A2). A second AMI, composed of the lateral gastrocnemius and the tibialis anterior, was designed to control the bionic ankle joint, responsible for prosthetic plantar flexion and dorsiflexion movements (Fig. 1,

A3 and A4). In each AMI, each muscle was mechanically linked to its partner via a tendon, which passed through a synovial canal, harvested from the amputated ankle joint at the time of amputation. One synovial canal was anchored to the medial flat of the tibia for each AMI and served as a biological pulley for that AMI, enabling the tendon to slide relative to the anchored sheath such that force production in one muscle caused stretch in the other. The AMI muscles were surgically coapted (connected via suture) with each muscle set at its resting tension, such that the default sensory state of each AMI reflected a neutral joint position.

At about 1-year postoperation, ultrasound imaging was used to interrogate motion of each AMI during volitional cyclical movement of the phantom limb. Movement commands were communicated to the subject in terms of phantom limb motion ("dorsiflex your ankle"), rather than activation of a specific muscle ("contract your tibialis anterior"). Fascicle strains were estimated from ultrasound video, recorded from the antagonist muscle as the subject volitionally contracted the agonist. Electromyography (EMG) was simultaneously recorded from the contracting agonist. Ultrasound fascicle data showed physiologically relevant strains (up to 16%) in the antagonist during volitional activation of the agonist. Cross-correlation of the agonist-integrated EMG signal and antagonist fascicle strain showed a strong relationship between agonist muscle activation and antagonist muscle stretch, with a correlation coefficient of 0.94 for inversion (Fig. 1B) and 0.91 for plantar flexion (Fig. 1C). Coupled motion was also preserved during cyclical alternating contraction of the agonist and the antagonist muscles at both low and high frequencies (movie S1). Additional video was recorded with the ultrasound probe positioned adjacent to the synovial canals; these videos showed sliding along the medial tibia, confirming coupled movement within each AMI (movie S1).

Control architecture: Prosthesis not in the loop
All experiments were carried out using a prototype ankle-foot prosthesis with powered ankle and subtalar joints (see the "Prosthetic hardware design" section in the Supplementary Materials for a description of the robotic hardware). When the AMI subject (subject A) wishes to move the bionic limb, he contracts the AMI muscles associated with his intended motion. Muscle activation is estimated from EMG collected via four bipolar surface electrodes on the surface of the skin, where each electrode is affixed adjacent to one of the four muscles comprising the two AMIs. These estimates are used to independently control position and impedance (mechanical stiffness) of the prosthetic ankle and subtalar joints (for a complete discussion of EMG processing and efferent control architecture, see the "Efferent control architecture" section and fig. S1). Because the AMI agonist and antagonist muscles are mechanically coupled within the residual limb of our subject, volitional contraction of an agonist passively stretches that muscle's antagonist. The natural neural responses from muscle spindles within both muscles are then interpreted by the central nervous system as sensations of joint position and speed, associated with movement of the prosthesis (Fig. 2A). During volitional movement of his phantom limb, subject A reported natural proprioceptive sensation throughout his phantom joint space, closely matching movement of the prosthesis.

In this free-space control architecture, there is no direct feedback line from the prosthesis to the AMI (hence, "prosthesis not in the loop"). However, the subject receives proprioceptive afferent feedback describing his intended movement command through agonist-antagonist
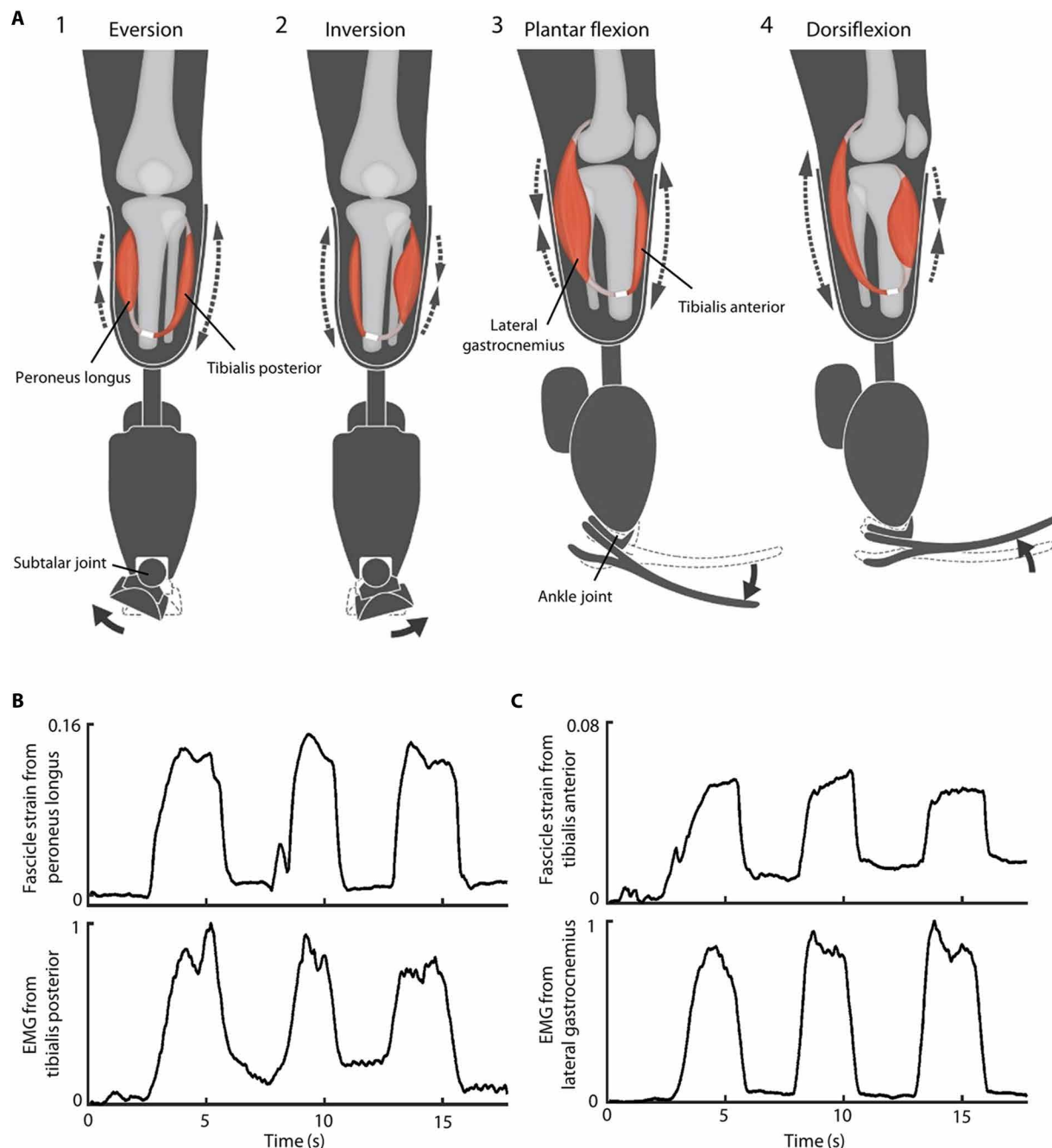
Fig. 1. Agonist-antagonist myoneural interface. (**A**) Two AMIs were surgically constructed within the left leg residuum of a patient to enable control of prosthetic subtalar and ankle joint movements. Prosthetic subtalar and ankle movements are shown in (A1) and (A2), and (A3) and (A4), respectively. In (A1), the prosthetic subtalar joint everts (arrow) when the peroneus longus contracts, stretching the tibialis posterior; in (A2), the subtalar joint inverts (arrow) when the tibialis posterior contracts, stretching the peroneus longus. In (A3), the prosthetic ankle joint dorsiflexes (arrow) when the tibialis anterior contracts, stretching the lateral gastrocnemius; in (A4), the ankle joint plantar-flexes (arrow) when the lateral gastrocnemius contracts, stretching the tibialis anterior. Dashed arrows indicate muscle contraction and stretch. (**B**) Ultrasound strain and EMG data for the subtalar AMI, showing coupled motion when the peroneus longus is stretched during volitional contraction of the tibialis posterior [inversion movement (A2)]. The correlation coefficient of these two signals is 0.94. (**C**) Ultrasound strain and EMG data for the ankle AMI, showing coupled motion when the tibialis anterior is stretched during volitional contraction of the lateral gastrocnemius [plantar flexion movement (A4)]. The correlation coefficient of these two signals is 0.91. (B) and (C) are representative traces from subject A (*n* = 5 trials per motion). EMG values are normalized to calibrated maxima for each muscle.

stretch relationships within the AMI. In free space, where no external torques are applied to the prosthetic joints, the efferent control system is designed to ensure that movement of the prosthesis is reliably synchronized with these natural afferent sensations; in this way, there is

limited functional difference between sensations of intended and actual joint motion.

Before beginning the experiments, we found that by tuning controller gains, we could adjust sensitivity of the prosthesis to make it
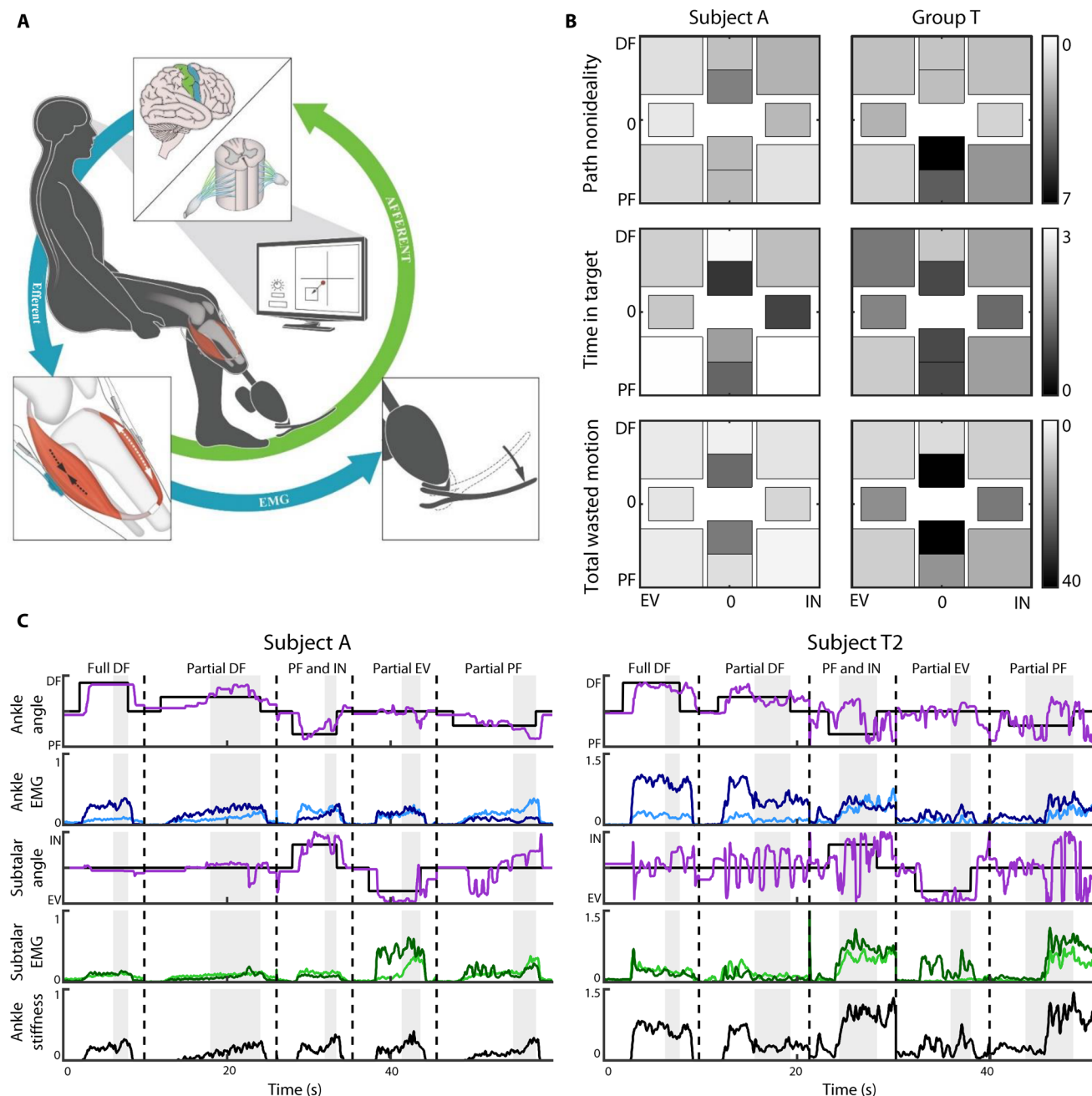
Fig. 2. Volitional control of joint position and impedance. (A) Schematic showing how subject A activates the AMI muscle associated with his intended motion. This activation is recorded as EMG and generates a movement command for the motors within the prosthesis. The subject can stiffen a prosthetic joint by simultaneously coactivating both the agonist and the antagonist muscles within the AMI associated with that joint. Afferent signals describing prosthetic joint movement are communicated to the patient's nervous system via muscle spindle response to differential stretch relationships within each AMI muscle. **(B)** Average performance maps for volitional control tasks (*n* = 100 samples from subject A, *n* = 350 samples from group T). The scores for each metric are presented by target area; the location of each rectangle within the axis represents the target area in joint space, ranging from full plantar flexion (PF) to full dorsiflexion (DF) and from full eversion (EV) to full inversion (IN). The shade of the rectangle indicates the subject's score in that target area, where lighter shades are indicative of better performance. **(C)** Representative sample traces of joint position (angle), EMG, and ankle stiffness during free-space volitional control experiments for subject A (*n* = 100 total samples) and one subject from group T (subject T2, *n* = 50 total samples). Dashed vertical lines divide the trial into segments by target motion, indicated by the text at the top of each segment. The shaded region of each plot represents the portion of that trial in which the subject was instructed to stiffen the joint. The range of ankle angles shown is the full range of the prosthetic ankle: from 15 degrees of PF to 10 degrees of DF. The range of subtalar angles shown is the full range of the prosthetic subtalar: from 15 degrees of EV to 15 degrees of IN. Ankle and subtalar angle plots show target position (black) and actual position (purple). The ankle EMG plot shows signal recorded from the lateral gastrocnemius (light blue) and the tibialis anterior (dark blue). The subtalar EMG plot shows signal recorded from the tibialis posterior (light green) and the peroneus longus (dark green). EMG values are normalized to calibrated maxima for each muscle. Stiffness values are normalized such that a value of 1 represents coactivation of the tibialis anterior and the lateral gastrocnemius at each muscle's calibrated maximum.

more or less reactive to muscle activity than the phantom limb. If the gains were too high, our subject described movement of the prosthesis as "jumpy." Conversely, if they were too low, he described the prosthesis as "sluggish" and "nonresponsive." Once the gains were well tuned, movement of the prosthesis and perceived movement of the phantom limb came into alignment. Control subjects having traditional unilateral transtibial amputation (group T), using the same prosthesis under identical conditions, did not report similar sensations. Despite ample gain adjustments and tuning, none of the control subjects felt that motion of the prosthetic joints closely matched sensation in the phantom limb. One subject (subject T2) specifically attributed this discrepancy in part to an unintended simultaneous antagonistic cocontraction during volitional activation of muscles within his residuum. All subjects in group T described a perception of limited motion throughout their phantom joint space.

Independent control of joint position and impedance

For all subjects, volitional control experiments were carried out after about 1 hour of tuning and free control of the device. These experiments evaluated each subject's ability to independently modulate prosthetic joint position and impedance while performing volitional control tasks with the prosthesis in free space. A graphical interface was generated to visualize prosthesis joint angles in real time as a point location in two-dimensional joint space (plantar flexion and dorsiflexion on the vertical axis and inversion and eversion on the horizontal). While wearing the prosthesis and watching the graphical interface, each subject was instructed to complete the following tasks: (i) move the prosthesis to within a predetermined window of joint angles, represented graphically as a rectangle in joint angle space; (ii) hold the prosthesis within this joint angle window for 3 s; (iii) stiffen the prosthesis by cocontracting the AMI muscles, while maintaining the joint position within the joint angle window; and (iv) return the prosthesis to its rest position.

After being introduced to the experimental paradigm and allowed one practice attempt, each subject repeatedly performed tasks 1 to 4 at 10 different locations across the full prosthesis joint angle space, in a randomly generated order. All trials were carried out within the same 2-hour session. Three metrics were selected to evaluate performance during volitional control experiments. For each metric, each subject's average performance was calculated across all trials performed by that subject to give an overall subject score. Scores for subject A (n = 100 samples from 10 trials) were compared to the average of the four subject scores from group T (n = 350 samples from 35 trials).

Identical experiments were also performed on a cohort of limbs with intact biological anatomy (n = 390 samples from 39 trials). This cohort included three of the four unaffected limbs from subjects in group T, as well as one limb of an additional subject with two intact biological limbs. For these experiments, subjects controlled the prosthesis with EMG signals measured from surface electrodes placed over the muscles in their intact biological limb. In this way, the performance metrics for this cohort are not meant to characterize the fully biological control system, but instead to capture performance of ideal muscular anatomy working in concert with the designed robotic platform. In addition, scores from subject A's unaffected leg (n = 100 samples from 10 trials) were compared with scores from the intact limb cohort to account for the possibility that subject A was uncharacteristically skilled at the particular experimental task.

The performance metrics used to assess volitional prosthetic control were path nonideality, time in target, and total wasted motion. All subjects successfully completed all tasks at all locations, with some target locations consistently more difficult than others (Fig. 2B; performance metrics for each individual subject are reported in table S1).

Path nonideality indicates the distance in angle space traversed by the prosthetic joints during the initial movement of the prosthesis from the rest angle to the target angle (task 1), normalized to the ideal distance from the rest angle to the center of the target square. Better performance in this metric is indicated by a lower score. Subject A's path nonideality score was 1.65 compared to an average score of 2.7 (±0.45) for subjects in group T. This represents a 39% improvement in performance. The average path nonideality score for the intact limb cohort was 1.68 (±0.87), and the score for subject A's unaffected limb was 1.56.

Time in target indicates ability to hold the prosthesis in the target window and is reported as the total time for which each subject maintained the prosthesis within the target during the 3-s hold task (task 2). Better performance in this metric is indicated by a higher score. Subject A's time in target score was 2.04 s compared to an average score of 1.53 s (±0.30) for subjects in group T. This represents a 33% improvement in performance. The average time in target score for the intact limb cohort was 2.16 s (±0.33), and the score for subject A's unaffected limb was 2.49 s.

Total wasted motion provides insight into stability and movement efficiency during joint motion and stiffening throughout all active portions of the trial (tasks 1 to 3). This is reported as the total angle-space distance traversed by the prosthetic joints, normalized to the minimum travel distance required to complete the tasks. Better performance in this metric is indicated by a lower score. Subject A's total wasted motion score was 7.45 compared to an average score of 21.74 (±2.68) for subjects in group T. This represents a 66% improvement in performance. The average total wasted motion score for the intact limb cohort was 8.79 (±3.17), and the score for subject A's unaffected limb was 7.33.

The representative sample traces in Fig. 2C qualitatively highlight the improved stability and path efficiency of subject A compared to subjects in group T during these volitional control experiments. These trends were also apparent in gait-related tasks requiring volitional control (Fig. 3 and movie S2). While wearing the prosthesis, subject A and each subject from group T were asked to step on the side of a 4-cm block placed in their path, such that the lateral edge (outside) of the prosthetic foot was in contact with the block, whereas the medial edge (inside) of the foot remained in contact with the floor. The block was placed on the floor at the location of expected foot strike of the subject's affected leg to force the prosthetic foot into an everted position (Fig. 3). All subjects were uniformly instructed to volitionally move the prosthetic ankle and subtalar joints during the swing phase of a single step such that the prosthetic subtalar would be everted appropriately for contact with the block. In subject A, we observed volitional repositioning of the subtalar into full eversion during the swing phase, consistent across all trials (n = 10). Swing-phase behaviors within group T were nonuniform, with high intersubject variability (n = 32 trials). Late swing eversion, defined as the maximum eversion angle achieved between 80 and 100% of the swing phase, was calculated for each trial. These values were then averaged to give an overall subject score. Subject A averaged 8.8 degrees of eversion, whereas the average score for group T was 4.8 (±5.9) degrees of inversion. Summary data are reported in Table 1.

Reflexive behaviors

Reflexive activity was evaluated during stair ascent and descent tasks, in which humans reflexively modulate swing-phase joint angle (*42*, *43*).
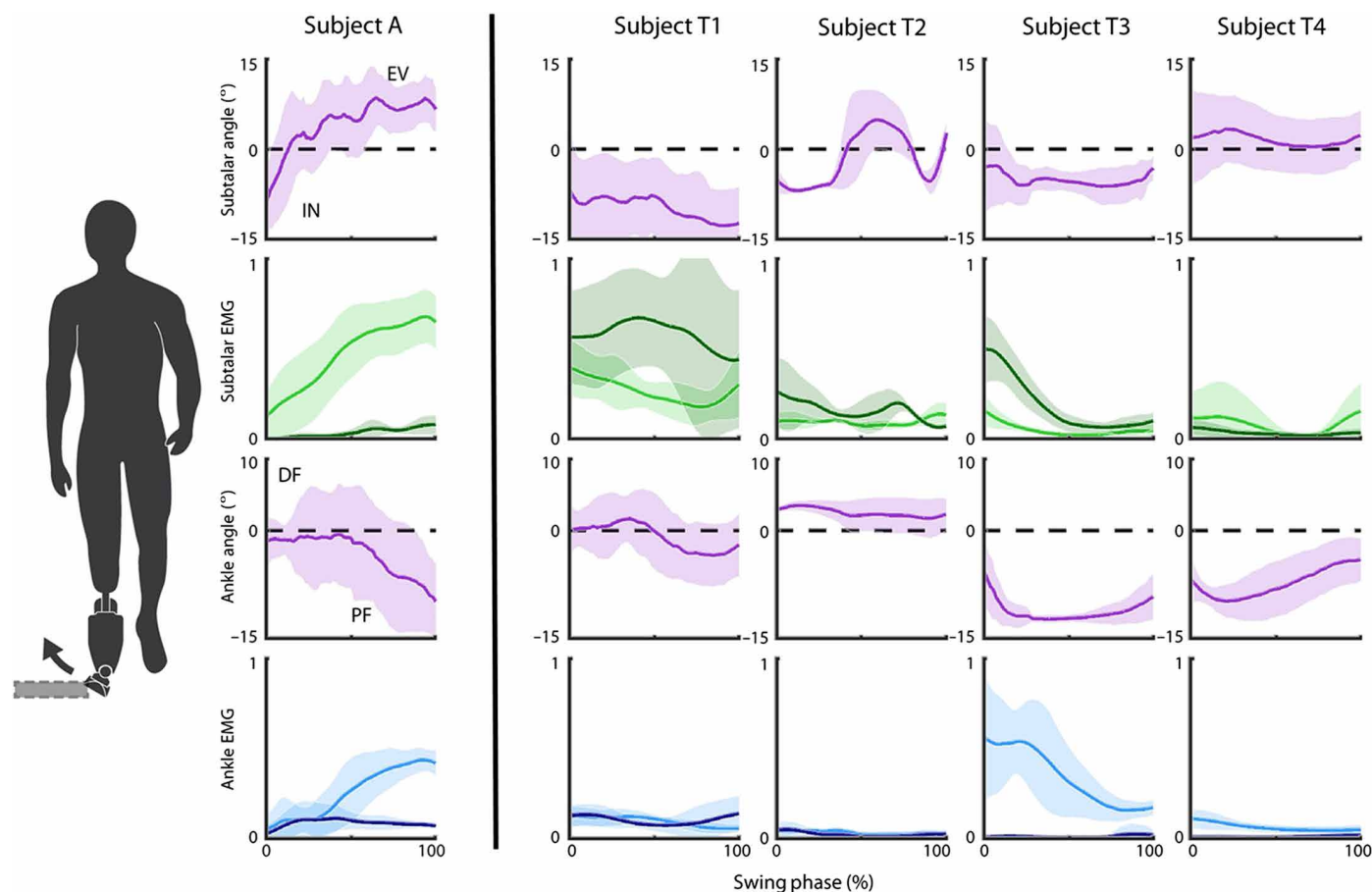
Fig. 3. Simultaneous subtalar and ankle control during a gait task requiring volitional eversion. Joint position and EMG during the swing phase of gait, as subject A (*n* = 10 trials) and each subject from group T (*n* = 32 trials) step onto the side of a block positioned on the floor to require eversion (arrow) of the prosthetic subtalar joint, as shown in the schematic. Shaded traces indicate mean ± 1 SD. Positive and negative subtalar angles correspond to eversion (EV) and inversion (IN), respectively. Positive and negative ankle angles correspond to dorsiflexion (DF) and plantar flexion (PF), respectively. The subtalar EMG plot shows signal recorded from the peroneus longus (light green) and the tibialis posterior (dark green). The ankle EMG plot shows signal recorded from the lateral gastrocnemius (light blue) and the tibialis anterior (dark blue). EMG values are normalized to calibrated maxima for each muscle.

Subject A and all subjects from group T were instructed to walk as naturally as possible and to avoid active volitional movement of the prosthesis. Instructions were carefully designed and delivered uniformly with intent to be clear, concise, consistent, and free from bias. While ascending stairs, subject A (*n* = 10 trials) first reflexively plantar-flexed the prosthetic ankle as the prosthesis left the ground and then dorsiflexed during swing to appropriately position the foot before placing it on the step (Fig. 4A and movie S3). He described these actions as automatic. These behaviors were not observed in subjects from group T (*n* = 32 trials). Late swing dorsiflexion, defined as the maximum dorsiflexion angle achieved between 80 and 100% of the swing phase, was calculated for each trial, and comparisons were made as above. Subject A averaged 7.3 degrees of dorsiflexion compared to 7.0 (±3.8) degrees of plantar flexion in group T. Summary data are reported in Table 1.

While descending stairs (prosthetic leg leading), subject A exhibited plantar flexion in late swing to prepare for foot-ground contact (Fig. 4B and movie S3). This behavior is fundamental to normalized stair-descent gait (*42, 43*). Late swing plantar flexion was not appreciable in three of the four subjects from group T. The fourth subject

(T3) consistently plantar-flexed beginning before toe-off, and the degree of plantar flexion lessened as the subject moved through the swing phase. Late swing plantar flexion was defined as the maximum plantar flexion angle achieved between 80 and 100% of the swing phase. Subject A averaged 11.9 degrees of plantar flexion compared to 2.3 (±3.2) degrees of plantar flexion in group T. Summary data are reported in Table 1.

Control architecture: Prosthesis in the loop

The final set of experiments was designed to evaluate whether FES can provide usable torque information from the prosthetic device to a subject having AMIs. To close the control loop around the prosthesis, afferent feedback of prosthetic joint torque was provided to subject A through stimulation of the AMI muscles (Fig. 5A). In response to torque measured on the prosthesis, microprocessors on the bionic leg commanded artificial stimulations to the antagonist muscle within each AMI, controlling the force borne on the mechanically coupled agonist. To validate this feedback modality in isolation, stimulation was first applied to the tibialis anterior—the muscle linked to prosthetic dorsiflexion—in absence of the prosthesis. Subject

Clites *et al.*, *Sci. Transl. Med.* **10**, eaap8373 (2018)   30 May 2018

6 of 13

Table 1. Summary data for terrain traversal trials. The metric in the second column was calculated for each trial of the task named in the first column and averaged within each subject to give an overall subject score. Subject A's overall subject score for each task (from *n* = 10 trials per task) is reported in the third column. The fourth column reports mean ± 1 intersubject SD for group T (*n* = 4 subjects, *n* = 32 total trials per task). Late swing eversion, late swing dorsiflexion, and late swing plantar flexion were calculated as the maximum eversion, dorsiflexion, and plantar flexion angles, respectively, achieved between 80 and 100% of the swing phase of the relevant task.

Task	Metric	Subject A (*n* = 1)	Group T (*n* = 4)
Eversion block	Late swing eversion	8.8 degrees of eversion	4.8 (±5.9) degrees of inversion
Stair ascent	Late swing dorsiflexion	7.3 degrees of dorsiflexion	7.0 (±3.8) degrees of plantar flexion
Stair descent	Late swing plantar flexion	11.9 degrees of plantar flexion	2.3 (±3.2) degrees of plantar flexion

A qualitatively described the sensation associated with this stimulation as "standing at the edge of a step, with [his] weight pushing down," forcing his phantom ankle into a dorsiflexed state. By volitionally activating his calf muscles, he counteracted the perceived dorsiflexion and felt the phantom ankle return to a neutral position, as if he had done a calf-raise exercise while still standing at the step's edge. Subject A acknowledged the absence of cutaneous sensation and described perceiving the stimulation as "involuntary contraction" in the artificially stimulated tibialis anterior. However, he felt that these were minor distractions, to which he would grow accustomed with repeated use of the prosthesis.

Characterization of perception

Two psychometric evaluations were performed to quantify subject A's perception of torque intensity in absence of the prosthesis. First, a magnitude estimation experiment was carried out in a manner similar to experiments previously described in the literature (*19*, *25*). Stimulation was delivered to the tibialis anterior at randomly selected current amplitudes of integer values between 0 and 4 mA. Subject A was blinded to all stimulation parameters throughout the experiment. During each trial, the subject was instructed to remain at rest until he felt stimulation pulling his phantom ankle into a dorsiflexed position. He was then asked to counteract this perceived ankle torque by volitionally plantar-flexing his phantom ankle until the perceived joint angle returned to its neutral state. After stimulation had subsided, the subject verbally rated the magnitude of perceived torque (Fig. 5B). There was a significant correlation between perceived dorsiflexion torque and stimulation amplitude ($P < 0.0001$, $R^2 = 0.96$, $n = 25$).

In the second psychometric evaluation, a forced-choice paradigm was used to establish the just-noticeable difference (JND) for stimulation intensity, following the protocol outlined in (*25*). During each trial, a pair of stimuli were applied to the tibialis anterior in a pseudorandom order; one of the two stimuli was delivered at a reference amplitude (2 mA), and the other was delivered at 1 of 11 possible stimulus values ranging from 0 to 4 mA. Each pair of stimuli was presented a total of 20 times in a pseudorandomly generated order, for a total of 220 individual trials. After each pair was presented, subject A was asked to indicate which of the two stimuli he perceived as stronger. Both subject A and the experimenter were blinded to stimulus amplitudes. A cumulative normal distribution was fit to the raw discrimination data to obtain a psychometric function. Two estimates of JND were calculated from this function as the change in stimulus amplitude that resulted in 75% judgment accuracy: one for increases relative to the reference value and the other for decreases relative to the reference value. These two values were then averaged to give a single estimate of JND. The psychometric curve for subject A was smooth, and the JND specific to this reference amplitude was 0.065 mA (Fig. 5C).

Closed-loop torque control

Afferent feedback of prosthetic torque through stimulation of the AMI antagonist improved performance during torque control tasks. In these experiments, subject A plantar-flexed the prosthetic ankle in response to verbal commands of percent effort (25, 50, 75, and 100%), thereby applying torque to a linear rotary-spring foot pedal. Sample trial plots (Fig. 5D) show the relationship between EMG activity, torque measured on the foot pedal, and stimulation amplitude. Summary results from these experiments are shown in Fig. 5E. With stimulation, subject A consistently generated four distinct torques at each of the four effort levels ($P < 0.025$, Tukey-Kramer, $n = 79$). Without muscle stimulation feedback, the torques generated at 50 and 75% effort and 75 and 100% effort did not differ significantly ($P > 0.1$, Tukey-Kramer, $n = 79$). Torques produced at 25, 50, and 100% effort were significantly different between the stimulation on and stimulation off cases ($P < 0.02$, *t* test), whereas those produced at 75% effort did not show a significant difference ($P = 0.73$). In his unaffected limb, subject A generated significantly different torques at each of the four effort levels ($P < 0.001$, Tukey-Kramer, $n = 80$).

Descriptions of the control experience

After each session, study participants were asked to comment on the experience of controlling the prototype prosthesis. Subject A described feeling as if the prosthesis was "his leg," referring to his missing biological limb. He explained, "My [conventional] prosthesis doesn't have the same sort of animation to it. This feels like it's alive." Over the course of this study, we observed subject A's candid interactions with the prosthesis during experimental downtime. On one occasion, at the end of the first trial day, we noticed that he was unconsciously fidgeting with the prosthetic foot while seated and engrossed in conversation (movie S4). On the second trial day, after standing on the device for only a few minutes, we watched as he wiggled his prosthetic foot to dislodge a roll of tape that had adhered to the bottom of his shoe (movie S4). These small behaviors provide evidence to support the subject's claim that the prosthesis had become embodied. Two days after the first trial day, in an email sent spontaneously to the research team, subject A explained, "Two days later and what transpired is still slowly sinking in. I keep trying to describe the sensation to people. Then this morning [my daughter] asked me if I felt like a cyborg. The answer was 'no, I felt like I had a foot'. I think that in just the short time I had it wired in and mounted to me it was quickly becoming part of me."

Subjects from group T described a remarkably different subjective control experience. Subjects T1 and T4 both felt that their interaction with the device was similar to the interaction one might have playing a video game for the first time. Subject T2 explained that the prosthesis sometimes "behaved in a way that was somewhat surprising" and acknowledged that he felt "a bit of disconnect" with the device. He postulated that this disconnect would shrink over time, as
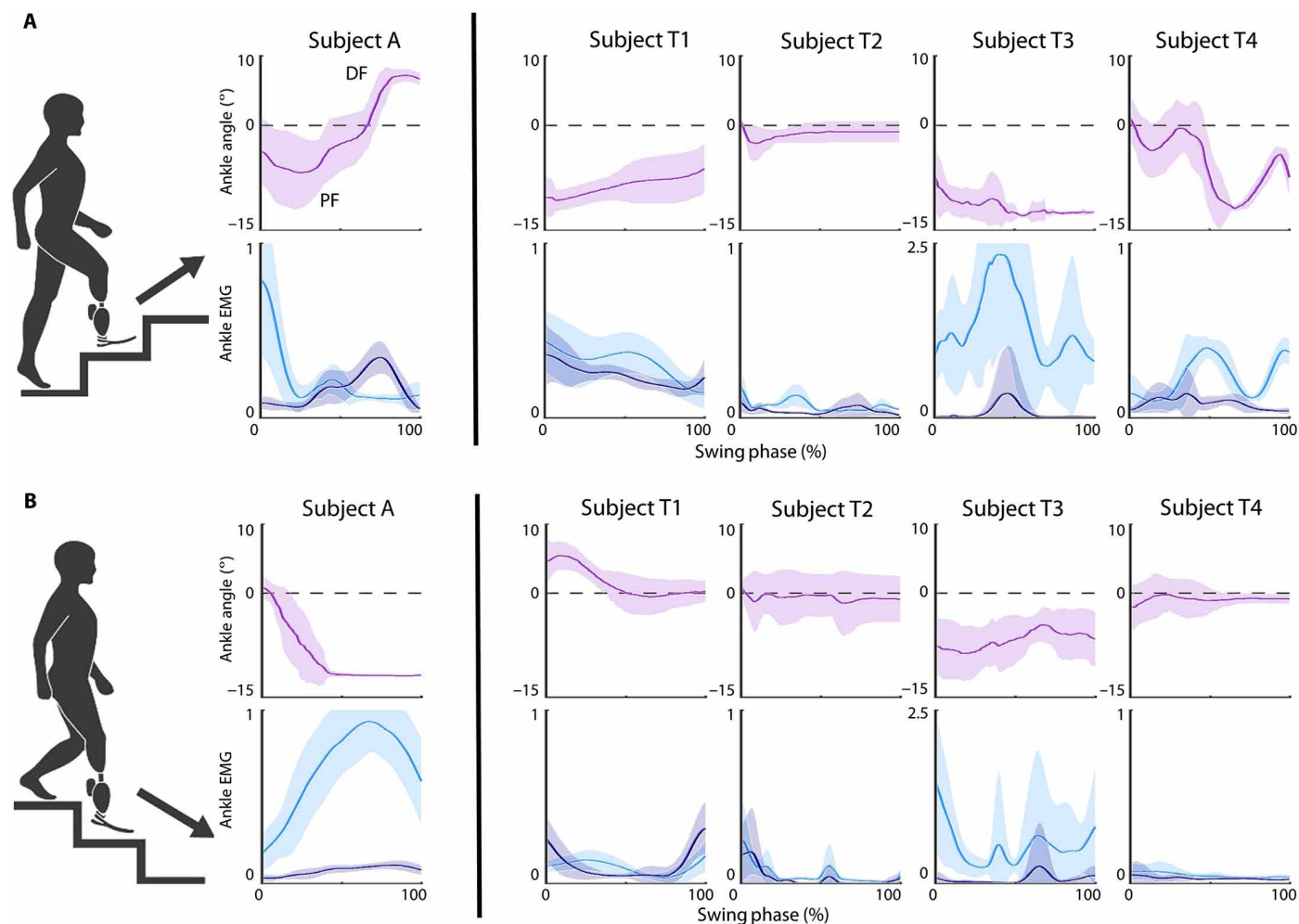
Fig. 4. Reflexive control during stair tasks. Ankle position and EMG while each subject (**A**) ascends and (**B**) descends stairs. Shaded traces indicate mean ± 1 SD for subject A (n = 10 trials for each of ascent and descent) and each subject from group T (n = 32 trials for each of ascent and descent). The ankle EMG plots show signal recorded from the lateral gastrocnemius (light blue) and the tibialis anterior (dark blue). Arrow indicates direction of movement. EMG values are normalized to calibrated maxima for each muscle.

he learned to control the joints in a more predictable way. Upon further questioning, he revealed that his connectedness with any prosthesis was directly linked to the "sensation he received from it." Although this subject was pleased to be able to feel the device moving, which he perceived through shifts in momentum and vibrations carried through his socket, he noted that these sensations were only present while the joints were in motion. In his words, "I can feel it in the passage from point A to point B, but once it's at point B, or once it's resting at point A, there's no sensation." Subject T3 described "not really trusting" the device. Universal to the correspondence of subjects from group T was a distinct lack of ownership of the prosthesis or emotion associated with controlling it. The discrepancy in experience between subject A and group T may highlight the fundamental role of natural afferent sensation in prosthesis embodiment (*44–47*).

DISCUSSION

Proprioceptive sensation pertaining to a synthetic appendage was reflected onto the nervous system of a subject with two AMIs surgically

constructed in his transtibial residuum. This subject (subject A) showed improved stability and motion path efficiency in free-space volitional control tasks, as compared to the cohort of four subjects having traditional transtibial amputation (group T). While ascending and descending stairs, subject A also demonstrated reflexive swing-phase behaviors that were absent in group T. In addition, we characterized a methodology for closed-loop torque control with afferent proprioceptive feedback of joint torque from a prosthetic limb in persons having one or more AMIs. This feedback improved performance on torque control tasks.

One possible explanation of performance gaps between subject A and group T during volitional control tasks is a lack of fine control over residual muscle activation in the latter group. Several of the subjects in group T described involuntary cocontraction as a prominent source of efferent control difficulty; accompanying volitional activation of a muscle in the residual limb is a consistent unintended contraction in that muscle's antagonist. Consequently, these subjects must increase the volitional activation of their agonist to overpower the unintended antagonistic activation. This likely played a role in a
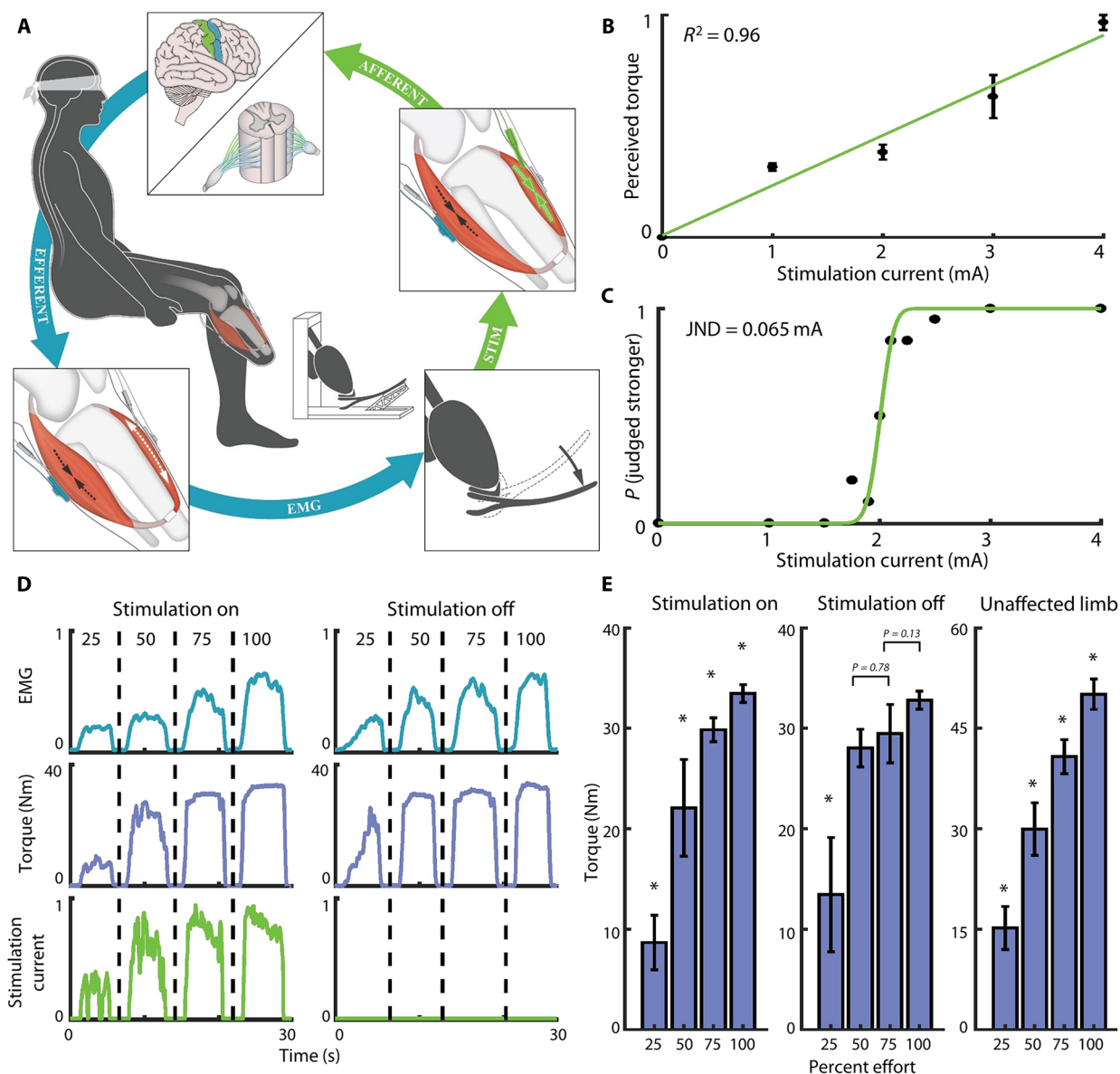
Clites *et al.*, *Sci. Transl. Med.* **10**, eaap8373 (2018)   30 May 2018

8 of 13

Fig. 5. Closed-loop torque control. (**A**) Schematic of the prosthesis-in-the-loop control architecture, in which afferent feedback of prosthetic joint torque is provided via FES of the antagonist muscle. The patient perceives this stimulation as a natural sensation of ankle torque. (**B**) Magnitude estimation of perceived dorsiflexion torque as a function of stimulation current delivered to the tibialis anterior. Perceived torques are normalized to the maximum reported value. For clarity in plotting, each point represents the mean value of five independent trials. Error bars represent the SE, and the R^2 coefficient reported on the plot is that of the mean values. (**C**) Discrimination performance as a function of differences in stimulation current. The reference current for all forced choice trials was 2 mA. Points indicate percentage of test stimuli correctly identified as stronger or weaker than the reference over 20 pairwise trials, and the green line represents a cumulative normal distribution fit to the raw data. (**D**) Representative sample traces of lateral gastrocnemius EMG (blue), torque (purple), and stimulation current (green) during closed-loop torque control trials for the "stimulation on" ($n = 79$ total trials) and "stimulation off" ($n = 79$ total trials) cases. Numbers at the top of the plot correspond to percent effort commands. Stimulation currents are normalized to 9 mA. EMG values are normalized to calibrated maxima for each muscle. (**E**) Summary data for closed-loop torque control trials in each of the stimulation on ($n = 79$ trials), stimulation off ($n = 79$ trials), and "unaffected limb" ($n = 80$ trials) cases. An asterisk above a bar indicates that the bar is significantly different from all other bars in the plot ($P < 0.025$). Where no significance was seen, a P value for the comparison is shown. Error bars represent a 99.9% confidence interval on the mean.

perception that EMG output was binary (on or off) and in the instability that plagued all subjects in group T while attempting to generate graded volitional movement commands during the volitional control experiments.

Cocontraction during gait in patients having unilateral lower-extremity amputations has been documented in several independent studies (*48*, *49*). In these studies, it is hypothesized that cocontrac-

tion is the result of an effort to stabilize the residual limb within the prosthetic socket during the swing phase of gait. However, increased levels of involuntary cocontraction have also been observed in upper-extremity amputees during volitional control tasks (*50–52*). We posit that these complications may be attributed, at least in part, to limitations of the traditional clinical amputation procedure and rehabilitation protocol. Because the muscles in the residual limb of all subjects in

group T are anchored at fixed lengths, the dynamic muscle relationships that exist within a biological limb with intact anatomy are broken. These relationships are fundamental to fine motor control and functional joint stability (30, 53–55) and play a significant role in reciprocal reflex inhibition (56–58). In their absence, traditional inhibitory reflex arcs may be disrupted, which would increase unintended antagonistic coactivation, and have a profound impact on a patient's ability to generate independent and separable muscle commands. The AMI has the potential to resolve this limitation by restoring the agonist-antagonist muscle relationships that are essential to appropriate reflexive muscle activation and by providing feedback of movement commands in the form of proprioceptive sensation. Supported by ultrasound data and patient testimonials, it is our hypothesis that dynamic agonist-antagonist stretch relationships in the residuum of subject A provide a proprioceptive affirmation of muscle activity within his residuum; each time he seeks to move his phantom limb, subject A receives confirmation of correct muscle activation as stretch receptors within the AMI muscles send signals to his brain.

Swing-phase adjustments to joint position and impedance play a critical role in the adaptation of gait to varying terrains (42, 43), and their absence has a significant impact on gait symmetry (59, 60). Replicating these adaptations has long been a goal of lower-extremity prosthetic research, with the majority of efforts focused on intrinsic or EMG-based terrain prediction and recognition methodologies (61–63). Unfortunately, both the accuracy and versatility of these state-of-the-art approaches pale in comparison to the human central nervous system, with its unparalleled ability to synthesize data streams from a vast array of biological sensors into a cogent motor control framework. While traversing various terrains, subjects in group T did not consistently demonstrate reflexive swing-phase modulation of prosthetic joint angle that would result in natural gait adaptations. These findings are in line with several studies examining EMG profiles in persons having transtibial amputation. In one study, it was shown that there is little intersubject consistency in muscle activation profiles during level ground walking and that muscle recruitment patterns do not match those in persons with two intact biological limbs (49). In another study, it was concluded that persons having transtibial amputation are more prone to cocontraction within the residual ankle musculature than healthy controls (48), which is consistent with our observations in several subjects from group T. In contrast, subject A reflexively modulated swing-phase joint angle in a manner appropriate to each terrain without training. These findings underscore the potential of the AMI to reinstate the central nervous system as the primary mediator of gait adaptation by providing the afferent proprioceptive sensations that are crucial to this function.

Here, we characterize a methodology to communicate sensations of joint torque from a bionic limb directly to the nervous system in a patient having an AMI. This feedback is perceived by subject A as natural torque about his phantom ankle and improves his performance in a task requiring torque modulation. Reliable closed-loop control of joint torque has the potential to provide an array of functionality to prosthetic users that was heretofore impossible. However, for these visions to become a reality, it will be necessary to improve viability of the stimulation delivery mechanism. The fine-wire electrodes used in this study are not a feasible long-term solution, because they are placed acutely for each experimental session and are not sufficiently anchored within the muscle to withstand the large shear forces associated with socket use. These issues can be resolved with a shift to permanently implanted intramuscular or epimysial electrodes that are fixed in place on the muscle to deliver repeatable stimulation (16, 17). In addition, it is worth noting that stimulation of residual muscles may also improve performance during torque-control tasks in persons with traditional amputation; however, the mechanism behind any potential improvement resulting from such an approach, which would involve stimulating muscles that are fixed isometrically, would fundamentally differ from the agonist-antagonist relationships that drive perception within the natural limb.

Another key difference between the experiences of subject A and group T is rooted in their subjective descriptions of their relationship with the prosthesis. Subject A felt an immediate and lasting connection with the device, whereas subjects in group T described a distinct disconnect. On the basis of their accounts, we believe that the difference in embodiment is attributable to two primary factors, namely, (i) robustness and intuitiveness of efferent control and (ii) reliability of afferent feedback. It is our position that each correctly executed volitional or reflexive behavior, reinforced by natural proprioceptive sensation, has the potential to deepen the relationship between human and machine. In this way, a bionic system that integrates more completely with a patient's sense of self has the potential to improve usage and satisfaction (44).

In this case study, the AMI described was implemented in an ideal surgical setting. The elective nature of the amputation made it possible to carefully plan our surgical approach. The muscular anatomy and limited degrees of freedom of the ankle and subtalar joints simplified the procedure relative to what would be necessary at the above-knee level or in the upper extremity. Even the patient's indication for amputation was advantageous; nonresolving bone injury represents an optimal availability of healthy distal soft tissue. However, it is important to note that the benefits of the AMI are not restricted to this limited patient population. Research is already underway to explore construction of AMIs at other amputation levels, as well as in the upper extremity. A recent study demonstrated the potential to leverage regenerative capabilities of nerve and muscle tissue in the construction of AMIs in settings where distal tissues are no longer available, such as traumatic amputations or revisions to existing amputations (40). It is worth noting that, even with these advancements, the implementation of the AMI may not be appropriate in patients requiring amputation due to advanced peripheral vascular disease. Patients in this population typically exhibit neuropathy and microvascular compromise, which may negate the benefits of the AMI and inhibit proper wound healing. Nevertheless, even if this population were excluded entirely, a majority of the remaining estimated 46% of patients indicated for amputation (64) would be eligible for an AMI procedure. It is also noteworthy that the study presented herein does not separate the impact of the AMI procedure from the visualization exercises that were added to the rehabilitation protocol with the intent of preserving muscle sliding (for details, see the "Subject selection, surgery, and rehabilitation" section). This is a feature inherent to a case study design that relies on a historic control group. Because this is a first-in-human case study, the results presented herein serve to highlight the potential of the AMI to improve volitional and reflexive neural control of a prosthetic device; a larger trial in a greater number of patients is necessary to definitively understand the degree of improvement that can be attributed specifically to the AMI procedure.

Proprioceptive insensibility has long been a stumbling block for integration of bionic devices with human physical identity. The AMI is fundamentally distinct from other approaches in that its implementation begins with a reengineering of the musculoskeletal anatomy

within the residuum. This approach is built upon an expanded understanding of what comprises a "neural interface" to incorporate not only synthetic components but also biological tissues (26, 65). Because of the inherent capacity of muscle tissue to amplify efferent neural signals and mechanoreceptors within muscle and tendon to communicate afferent proprioceptive information to the nervous system, these native biological transducers are ideally suited to act as the bidirectional interface between the nerve and the prosthesis. The AMI was designed with the intent of optimizing this biological interface. The results presented herein demonstrate the potential of such a bionic system to improve functional outcomes and embodiment when compared with a traditional approach to amputation.

MATERIALS AND METHODS
Study design
The primary hypothesis investigated in this case study is that the AMI procedure and rehabilitation protocol (i) enables independent control of prosthetic joint angle and impedance and (ii) reflects proprioceptive afferent sensation pertaining to each joint of a two-degree-of-freedom ankle-foot prosthesis onto the central nervous system. The experiments presented were designed to demonstrate the AMI's potential to improve volitional, free-space control, restore swing-phase reflexes while traversing various terrains, and perform closed-loop torque control tasks. This was a first-in-human, nonrandomized case study. The experimental subject (subject A) served as his own control where possible. Where control subjects having a traditional amputation were needed, four subjects were selected (group T), representing a wide array of patient demographics. None of the patients reported or showed signs of any complicating nerve or muscle damage within the residual limb.

Subject selection, surgery, and rehabilitation
The AMI operation and clinical follow-up were performed with informed consent at Brigham and Women's Hospital, under the approval of the Partner's Health System Institutional Review Board. All other experiments were carried out with informed consent at the Massachusetts Institute of Technology (MIT), under the approval of the Committee on the Use of Humans as Experimental Subjects. Subject A was selected for participation based primarily on his need for elective unilateral transtibial amputation, indicated due to a traumatic Hawkins type 4 talus fracture and persistent nerve pain. He was 53 years old at the time of his primary amputation in July 2016. During this primary amputation, two AMIs were constructed within his residual limb by one of the study authors (M.J.C.). The amputation osteotomy was performed at 12 cm distal to the patellar ligament, resulting in a residuum of standard length. Acute rehabilitation began at 6 weeks postoperation. In addition to standard rehabilitation protocols, the patient regularly performed exercises focused on preserving motion within the AMI constructs. During these exercises, the patient was asked to visualize his phantom limb and focus on moving his phantom foot through the four primary ankle and subtalar joint motions (plantar flexion and dorsiflexion, inversion and eversion). No direct feedback of muscle activity was provided to the patient during rehabilitation exercises. Experimental sessions with the bionic prosthesis began in late April 2017 (9 to 10 months postoperation) and continued through November 2017 (16 to 17 months postoperation).

All subjects in group T were men with unilateral transtibial amputation, selected to incorporate a range of patient age (range, 37 to 47 years), time since amputation (range, 1 to 24 years), and body mass index (range, 24 to 33 kg/m²). For more details about these subjects, see the "Subject selection (group T)" section in the Supplementary Materials.

Surface electrode placement and EMG processing
EMG was recorded via bipolar surface electrodes, placed acutely over each of the four target muscles: lateral gastrocnemius for plantar flexion, tibialis anterior for dorsiflexion, tibialis anterior for inversion, and peroneus longus for eversion. An identical electrode placement protocol was followed for all experimental subjects. For further details, see the Supplementary Materials.

Efferent control architecture
The efferent control paradigm explored in this study was designed to allow direct control of prosthetic joint position and impedance. In this control approach, EMG signal amplitudes recorded from the agonist and antagonist AMI muscles were interpreted as desired torques produced in opposite directions about a virtual dynamic joint, which was constructed with physiologically relevant values for virtual parallel spring stiffness, virtual damping, and virtual inertia. The difference of these estimated torques was then applied to the virtual joint, causing it to move. The position of the virtual joint controlled the desired position of the associated prosthetic joint (fig. S1). Prosthetic joint stiffness was directly modulated by the mean activation of the agonist and antagonist muscles, as modeled in (53). This control architecture enables independent modulation of joint position and impedance. As with all EMG-based proportional control systems, there is a trade-off between joint stability and latency; typically, the particulars of this trade-off are buried in filter design. One benefit to the virtual-joint architecture is that filter parameters take on intuitive physical meaning and can be set to near-physiologic values. For a description of controller tuning, see the Supplementary Materials.

Although stimulation was active for prosthetic joint torque feedback, the stimulated muscle was assumed to be at zero activation, and input from that muscle to the controller was blocked (fig. S1). Although this design eliminates the ability to actively move the joint in the same direction as an applied load, the scenarios in which this action would be desirable are likely to be extremely limited.

Fine-wire electrode placement and stimulation
Fine-wire electrodes were placed acutely (M.J.C.) at the start of each trial day, according to the technique presented in (66). For all trials, the tibialis anterior muscle was stimulated with a 50-Hz, current-controlled, charge-balanced, asymmetric, biphasic pulse train (NL800, Digitimer). The pulse width of the cathodic phase was 200 μs and that of the anodic phase was 400 μs. For the closed-loop torque control experiments, the cathodic current amplitude was modulated in linear proportionality to prosthetic torque (measured or simulated) and ranged from 0 to 9 mA. For a full description of the electrode placement protocol, stimulation parameters, and evidence of proper electrode placement, see the Supplemental Materials, fig. S2, and movie S5.

Closed-loop torque control experimental setup
During the closed-loop torque control experiments, the prosthesis was mounted to an assembly that held it in contact with the foot pedal, remote from the subject, to eliminate the possibility of confounding force feedback through the prosthetic socket. The subject

was acoustically isolated with noise-canceling headphones worn over ear plugs and visually isolated with a sleep mask. He performed eight total trial groups under two different conditions; four of these trial groups were performed with torque feedback through stimulation of the AMI, and four were performed without such stimulation. Under the stimulation on condition, the tibialis anterior was stimulated with a current amplitude proportional to the plantar flexion torque measured on the prosthesis. Under the stimulation off condition, no such feedback was provided. Each trial group consisted of 20 commands (5 at each effort level), presented in a random order. Within a single trial group, all trials were carried out under the same condition, but the order of trial group conditions was selected at random. This format was chosen to account for bias in one condition having been consistently evaluated before the other, while preventing the possible scenario in which the subject applies excess torque in anticipation of a stimulus that never comes. The experiment was repeated without stimulation in subject A's unaffected limb to set a performance baseline. In these trials, subject A applied torque to the pedal with his right biological foot directly contacting the pedal. Pedal torque was streamed from the pedal's load cell to a data acquisition system (USB-6009, National Instruments).

Statistical analysis

Time-synchronized joint angle, EMG, and joint stiffness data were collected from the prosthesis in real time for all trials. Statistical comparisons were made within a given subject using the Tukey-Kramer multiple comparisons tests at a significance level of $\alpha = 0.025$. In cases where a single comparison was appropriate, a t test was used at a significance level of $\alpha = 0.025$. All statistical analysis was performed in MATLAB R2017a (The MathWorks). All EMG signals are normalized to calibrated maxima for each muscle. All shaded traces indicate mean ± 1 SD.

SUPPLEMENTARY MATERIALS

www.sciencetranslationalmedicine.org/cgi/content/full/10/443/eaap8373/DC1
Materials and Methods
Fig. S1. Control diagrams showing how EMG from the AMI muscles drives movement of the prosthetic joint.
Fig. S2. Raw EMG recorded from fine-wire electrodes during volitional movement of the phantom limb.
Movie S1. Ultrasound video of coupled AMI motion.
Movie S2. Volitional control.
Movie S3. Reflexive control.
Movie S4. Candid videos showing prosthesis embodiment.
Movie S5. Visual confirmation of stimulated muscle contraction.
Table S1. Individual subject data for volitional control tasks.

REFERENCES AND NOTES

1. U. Proske, S. C. Gandevia, The proprioceptive senses: Their roles in signaling body shape, body position and movement, and muscle force. *Physiol. Rev.* **92**, 1651–1697 (2012).
2. B. L. Riemann, S. M. Lephart, The sensorimotor system, Part II: The role of proprioception in motor control and functional joint stability. *J. Athl. Train.* **37**, 80–84 (2002).
3. E. R. Kandel, J. H. Schwartz, T. M. Jessell, in *Principles of Neural Science* (McGraw-Hill, 2013), vol. 4, 1414 pp.
4. J. J. Ochoa, E. E. Torebjörk, Sensations evoked by intraneural microstimulation of single mechanoreceptor units innervating the human hand. *J. Physiol.* **342**, 633–654 (1983).
5. G. Macefield, S. C. Gandevia, D. Burke, Perceptual responses to microstimulation of single afferents innervating joints, muscles and skin of the human hand. *J. Physiol.* **429**, 113–129 (1990).
6. D. F. Collins, K. M. Refshauge, G. Todd, S. C. Gandevia, Cutaneous receptors contribute to kinesthesia at the index finger, elbow, and knee. *J. Neurophysiol.* **94**, 1699–1706 (2005).
7. I. A. Boyd, T. D. M. Roberts, Proprioceptive discharges from stretch-receptors in the knee-joint of the cat. *J. Physiol.* **122**, 38–58 (1953).
8. S. Skoglund, Anatomical and physiological studies of knee joint innervation in the cat. *Acta Physiol. Scand. Suppl.* **36**, 1–101 (1956).
9. D. Burke, S. C. Gandevia, G. Macefield, Responses to passive movement of receptors in joint, skin and muscle of the human hand. *J. Physiol.* **402**, 347–361 (1988).
10. L. Jami, Golgi tendon organs in mammalian skeletal muscle: Functional properties and central actions. *Physiol. Rev.* **72**, 623–666 (1992).
11. G. Eklund, Position sense and state of contraction; the effects of vibration. *J. Neurol. Neurosurg. Psychiatry* **35**, 606–611 (1972).
12. G. M. Goodwin, D. I. McCloskey, P. B. C. Matthews, The contribution of muscle afferents to kinaesthesia shown by vibration induced illusions of movement and by the effects of paralysing joint afferents. *Brain* **95**, 705–748 (1972).
13. E. Ribot-Ciscar, J.-P. Roll, Ago-antagonist muscle spindle inputs contribute together to joint movement coding in man. *Brain Res.* **791**, 167–176 (1998).
14. B. J. Brown, M. L. Iorio, M. R. Klement, M. R. Conti Mica, A. El-Amraoui, P. D. O'Halloran, C. E. Attinger, Outcomes after 294 transtibial amputations with the posterior myocutaneous flap. *Int. J. Low. Extrem. Wounds* **13**, 33–40 (2014).
15. P. Cao, P. De Rango, in *Rutherford's Vascular Surgery* (Saunders Elsevier, 2010), vol. 2, pp. 1469–1486.
16. M. Ortiz-Catalan, R. Brånemark, B. Håkansson, J. Delbeke, On the viability of implantable electrodes for the natural control of artificial limbs: Review and discussion. *Biomed. Eng. Online* **11**, 33 (2012).
17. X. Navarro, T. B. Krueger, N. Lago, S. Micera, T. Stieglitz, P. Dario, A critical review of interfaces with the peripheral nervous system for the control of neuroprostheses and hybrid bionic systems. *J. Peripher. Nerv. Syst.* **10**, 229–258 (2005).
18. S. K. Au, J. Weber, H. Herr, Powered ankle–foot prosthesis improves walking metabolic economy. *IEEE Trans. Robot.* **25**, 51–66 (2009).
19. D. W. Tan, M. A. Schiefer, M. W. Keith, J. R. Anderson, J. Tyler, D. J. Tyler, A neural interface provides long-term stable natural touch perception. *Sci. Transl. Med.* **6**, 257ra138 (2014).
20. M. Ortiz-Catalan, B. Håkånsson, R. Brånemark, An osseointegrated human-machine gateway for long-term sensory feedback and motor control of artificial limbs. *Sci. Transl. Med.* **6**, 257re6 (2014).
21. S. Raspopovic, M. Capogrosso, F. M. Petrini, M. Bonizzato, J. Rigosa, G. Di Pino, J. Carpaneto, M. Controzzi, T. Boretius, E. Fernandez, G. Granata, C. M. Oddo, L. Citi, A. L. Ciancio, C. Cipriani, M. C. Carrozza, W. Jensen, E. Guglielmelli, T. Stieglitz, P. M. Rossini, S. Micera, Restoring natural sensory feedback in real-time bidirectional hand prostheses. *Sci. Transl. Med.* **6**, 222ra19 (2014).
22. M. A. Schiefer, D. Tan, S. M. Sidek, D. J. Tyler, Sensory feedback by peripheral nerve stimulation improves task performance in individuals with upper limb loss using a myoelectric prosthesis. *J. Neural Eng.* **13**, 16001 (2016).
23. K. Horch, S. Meek, T. G. Taylor, D. T. Hutchinson, Object discrimination with an artificial hand using electrical stimulation of peripheral tactile and proprioceptive pathways with intrafascicular electrodes. *IEEE Trans. Neural Syst. Rehabil. Eng.* **19**, 483–489 (2011).
24. G. S. Dhillon, K. W. Horch, Direct neural sensory feedback and control of a prosthetic arm. *IEEE Trans. Neural Syst. Rehabil. Eng.* **13**, 468–472 (2005).
25. E. L. Graczyk, M. A. Schiefer, H. P. Saal, B. P. Delhaye, S. J. Bensmaia, D. J. Tyler, The neural basis of perceived intensity in natural and artificial touch. *Sci. Transl. Med.* **8**, 362ra142 (2016).
26. T. A. Kung, N. B. Langhals, D. C. Martin, P. J. M. Johnson, P. S. Cederna, M. G. Urbanchek, Regenerative peripheral nerve interface viability and signal transduction with an implanted electrode. *Plast. Reconstr. Surg.* **133**, 1380–1394 (2014).
27. Z. T. Irwin, K. E. Schroeder, P. P. Vu, D. M. Tat, A. J. Bullard, S. L. Woo, I. C. Sando, M. G. Urbanchek, P. S. Cederna, C. A. Chestek, Chronic recording of hand prosthesis control signals via a regenerative peripheral nerve interface in a rhesus macaque. *J. Neural Eng.* **13**, 46007 (2016).
28. T. A. Kuiken, G. Li, B. A. Lock, R. D. Lipschutz, L. A. Miller, K. A. Stubblefield, K. B. Englehart, Targeted muscle reinnervation for real-time myoelectric control of multifunction artificial arms. *JAMA* **301**, 619–628 (2009).
29. L. J. Hargrove, A. M. Simon, A. J. Young, R. D. Lipschutz, S. B. Finucane, D. G. Smith, T. A. Kuiken, Robotic leg control with EMG decoding in an amputee with nerve transfers. *N. Engl. J. Med.* **369**, 1237–1242 (2013).
30. E. J. Rouse, L. J. Hargrove, E. J. Perreault, T. A. Kuiken, Estimation of human ankle impedance during the stance phase of walking. *IEEE Trans. Neural Syst. Rehabil. Eng.* **22**, 870–878 (2014).
31. H. M. Herr, A. M. Grabowski, Bionic ankle–foot prosthesis normalizes walking gait for persons with leg amputation. *Proc. Biol. Sci.* **279**, 457–464 (2012).
32. R. D. Bellman, M. A. Holgate, T. G. Sugar, SPARKy 3: Design of an active robotic ankle prosthesis with two actuated degrees of freedom using regenerative kinetics, in *Proceedings of the 2nd Biennial IEEE/RAS-EMBS International Conference on Biomedical Robotics and Biomechatronics, Biorob 2008* (IEEE, 2008), pp. 511–516.

33. F. Sup, A. Bohara, M. Goldfarb, Design and control of a powered transfemoral prosthesis. *Int. J. Rob. Res.* **27**, 263–273 (2008).

34. S. Huang, J. P. Wensman, D. P. Ferris, An experimental powered lower limb prosthesis using proportional myoelectric control. *J. Med. Device.* **8**, 24501 (2014).

35. H. Huang, T. A. Kuiken, R. D. Lipschutz, A strategy for identifying locomotion modes using surface electromyography. *IEEE Trans. Biomed. Eng.* **56**, 65–73 (2009).

36. L. J. Hargrove, A. M. Simon, R. D. Lipschutz, S. B. Finucane, T. A. Kuiken, Real-time myoelectric control of knee and ankle motions for transfemoral amputees. *JAMA* **305**, 1542–1544 (2011).

37. H. M. Herr, R. R. Riso, K. W. Song Jr., R. J. Casler, M. J. Carty, *Peripheral Neural Interface Via Nerve Regeneration to Distal Tissues* (Massachusetts Institute of Technology, 2016).

38. H. M. Herr, T. R. Clites, B. Maimon, A. Zorzos, M. J. Carty, J.-F. Duval, *Method and System for Providing Proprioceptive Feedback and Functionality Mitigating Limb Pathology* (Massachusetts Institute of Technology, 2016).

39. T. R. Clites, M. J. Carty, S. Srinivasan, A. N. Zorzos, H. M. Herr, A murine model of a novel surgical architecture for proprioceptive muscle feedback and its potential application to control of advanced limb prostheses. *J. Neural Eng.* **14**, 036002 (2017).

40. S. S. Srinivasan, M. J. Carty, P. W. Calvaresi, T. R. Clites, B. E. Maimon, C. R. Taylor, A. N. Zorzos, H. Herr, On prosthetic control : A regenerative agonist-antagonist myoneural interface. *Sci. Robot.* **2**, eaan2971 (2017).

41. T. R. Clites, M. J. Carty, H. M. Herr, *Plastic Surgery Research Council* (PSRC, 2017), 119 pp.

42. B. J. McFadyen, D. A. Winter, An integrated biomechanical analysis of normal stair ascent and descent. *J. Biomech.* **21**, 733–744 (1988).

43. R. Riener, M. Rabuffetti, C. Frigo, Stair ascent and descent at different inclinations. *Gait Posture* **15**, 32–44 (2002).

44. U. Wijk, I. Carlsson, Forearm amputees' views of prosthesis use and sensory feedback. *J. Hand Ther.* 269–277 (2014).

45. H. H. Ehrsson, B. Rosén, A. Stockselius, C. Ragnö, P. Köhler, G. Lundborg, Upper limb amputees can be induced to experience a rubber hand as their own. *Brain* **131**, 3443–3452 (2008).

46. A. Guterstam, V. I. Petkova, H. H. Ehrsson, The illusion of owning a third arm. *PLOS ONE* **6**, e17208 (2011).

47. M. Botvinick, J. Cohen, Rubber hands 'feel' touch that eyes see. *Nature* **391**, 756 (1998).

48. M. Seyedali, J. M. Czerniecki, D. C. Morgenroth, M. E. Hahn, Co-contraction patterns of trans-tibial amputee ankle and knee musculature during gait. *J. Neuroeng. Rehabil.* **9**, 29 (2012).

49. S. Huang, D. P. Ferris, Muscle activation patterns during walking from transtibial amputees recorded within the residual limb-prosthetic interface. *J. Neuroeng. Rehabil.* **9**, 55 (2012).

50. G. A. García, R. Okuno, in *Electrodiagnosis in New Frontiers of Clinical Research* (IntechOpen, 2013), pp. 269–285.

51. E. Scheme, K. Englehart, Electromyogram pattern recognition for control of powered upper-limb prostheses: State of the art and challenges for clinical use. *J. Rehabil. Res. Dev.* **48**, 643–660 (2011).

52. B. A. Lock, A. E. Schultz, T. A. Kuiken, Clinically practical applications of pattern recognition for myoelectric prostheses, in *Proceedings of the 2008 MyoElectric Controls/Powered Prosthetics Symposium* (MEC, 2008), pp. 0–5.

53. N. Hogan, Adaptive control of mechanical impedance by coactivation of antagonist muscles. *IEEE Trans. Automat. Contr.* **29**, 681–690 (1984).

54. H. Lee, N. Hogan, in *ASME 2010 Dynamic Systems and Control Conference* (ASME, 2010), pp. 6–8.

55. W. T. Edwards, Effect of joint stiffness on standing stability. *Gait Posture* **25**, 432–439 (2007).

56. A. M. Smith, The coactivation of antagonist muscles. *Can. J. Physiol. Pharmacol.* **59**, 733–747 (1981).

57. C. J. De Luca, B. Mambrito, Voluntary control of motor units in human antagonist muscles: Coactivation and reciprocal activation. *J. Neurophysiol.* **58**, 525–542 (1987).

58. M. Dimitriou, Human muscle spindle sensitivity reflects the balance of activity between antagonistic muscles. *J. Neurosci.* **34**, 13644–13655 (2014).

59. M. T. Nahorniak, G. E. Gorton III, M. E. Gannotti, P. D. Masso, Kinematic compensations as children reciprocally ascend and descend stairs with unilateral and bilateral solid AFOs. *Gait Posture* **9**, 199–206 (1999).

60. S. Sienko Thomas, C. E. Buckon, S. Jakobson-Huston, M. D. Sussman, M. D. Aiona, Stair locomotion in children with spastic hemiplegia: The impact of three different ankle foot orthosis (AFOs) configurations. *Gait Posture* **16**, 180–187 (2002).

61. H. Huang, F. Zhang, L. J. Hargrove, Z. Dou, D. R. Rogers, K. B. Englehart, Continuous locomotion-mode identification for prosthetic legs based on neuromuscular–mechanical fusion. *IEEE Trans. Biomed. Eng.* **58**, 2867–2875 (2011).

62. A. J. Young, T. A. Kuiken, L. J. Hargrove, Analysis of using EMG and mechanical sensors to enhance intent recognition in powered lower limb prostheses. *J. Neural Eng.* **11**, 56021 (2014).

63. R. Stolyarov, G. Burnett, H. Herr, Translational motion tracking of leg joints for enhanced prediction of walking tasks. *IEEE Trans. Biomed. Eng.* **65**, 736–769 (2017).

64. K. Ziegler-Graham, E. J. MacKenzie, P. L. Ephraim, T. G. Travison, R. Brookmeyer, Estimating the prevalence of limb loss in the United States: 2005 to 2050. *Arch. Phys. Med. Rehabil.* **89**, 422–429 (2008).

65. T. A. Kuiken, L. A. Miller, R. D. Lipschutz, B. A. Lock, K. Stubblefield, P. D. Marasco, P. Zhou, G. A. Dumanian, Targeted reinnervation for enhanced prosthetic arm function in a woman with a proximal amputation: A case study. *Lancet* **369**, 371–380 (2007).

66. T. A. Park, G. F. Harris, "Guided" intramuscular fine wire electrode placement: A new technique. *Am. J. Phys. Med. Rehabil.* **75**, 232–234 (1996).

Clites *et al.*, *Sci. Transl. Med.* **10**, eaap8373 (2018)   30 May 2018

13 of 13

Science Translational Medicine

Proprioception from a neurally controlled lower-extremity prosthesis

Tyler R. Clites, Matthew J. Carty, Jessica B. Ullauri, Matthew E. Carney, Luke M. Mooney, Jean-François Duval, Shriya S. Srinivasan and Hugh. M. Herr

A leg up for neuroprosthetics

Amputation severs bone, nerves, and muscles used for limb movement, limiting an amputee's ability to sense and control a prosthesis. Here, Clites *et al.* tested autologous muscle-nerve interfaces created at the time of below-knee amputation in a human subject. Compared to four subjects with traditional amputations, the subject who received two agonist-antagonist myoneural interfaces in his residuum (which were connected via synthetic electrodes to his powered prosthesis) exhibited greater joint placement control and reflexive behavior during stair walking. The subject noted little delay between intentional activation of the muscles in his residuum and movement of his prosthesis and expressed a strong sense of embodiment (identifying the prosthesis as part of him). Agonist-antagonist myoneural interfaces could help restore natural sensation to prosthetic joints.

ARTICLE TOOLS	http://stm.sciencemag.org/content/10/443/eaap8373
SUPPLEMENTARY MATERIALS	http://stm.sciencemag.org/content/suppl/2018/05/25/10.443.eaap8373.DC1
RELATED CONTENT	http://stm.sciencemag.org/content/scitransmed/10/432/eaao6990.full http://stm.sciencemag.org/content/scitransmed/8/362/362ra142.full http://stm.sciencemag.org/content/scitransmed/6/257/257ra138.full http://stm.sciencemag.org/content/scitransmed/6/222/222ra19.full http://stm.sciencemag.org/content/scitransmed/5/210/210ps15.full http://stm.sciencemag.org/content/scitransmed/6/257/257re6.full
REFERENCES	This article cites 56 articles, 7 of which you can access for free http://stm.sciencemag.org/content/10/443/eaap8373#BIBL
PERMISSIONS	http://www.sciencemag.org/help/reprints-and-permissions

Use of this article is subject to the Terms of Service